Reconfigurable Folded Reflectarray Antenna Based Upon Liquid Crystal Technology

Saygin Bildik, *Student Member, IEEE*, Sabine Dieter, *Member, IEEE*, Carsten Fritzsch, *Student Member, IEEE*, Wolfgang Menzel, *Fellow, IEEE*, and Rolf Jakoby, *Member, IEEE*

***Abstract*—A reconfigurable antenna based on the liquid crystal technology is presented in this paper. The antenna comprises a planar lower reflector with an incorporated feed at its center and a polarizing grid on top as an upper reflector. The lower reflector is utilized to collimate the beam and to twist the polarization. The polarizing grid selects the polarization for the transmission and reflects the orthogonally polarized waves toward the lower reflector. Combining reflector elements with a polarizing grid allows performing additional phase adjustment on the upper reflector for beam steering. Reconfigurability is maintained by the upper reflector, in which a liquid crystal mixture is used as a tunable substrate. The liquid crystal layer is tuned with a bias voltage configuration to obtain an appropriate phase adjustment for the beam steering. As a proof of concept, the beam steering capability of the antenna is demonstrated by steering the main beam to $-6°$, $0°$, and $6°$ at 78 GHz. The measured gain at 78 GHz is 25.1 dB. The proposed antenna configuration is a promising candidate for reconfigurable, high-gain, low-profile, and low-cost antennas.**

***Index Terms*—Beam steering, liquid crystals, microstrip antenna arrays, microwave antennas, millimeter wave technology, reflectarrays.**

I. Introduction

REFLECTOR antennas are always in the focus of interest for sensor and communication applications owing to high gain, low losses and low sidelobe levels. However, parabolic reflector antennas are sometimes costly to manufacture, and their high profile (together with the necessary feed) is not always compatible with space requirements, especially with mobile terminals, e.g., on vehicles, aircraft and spacecrafts, or with domestic applications. Microstrip patch arrays [1] are feasible for such kind of applications because of being planar, low-profile and lightweight. They are fabricated with a printed circuit technology that yields ease of fabrication and cost-effectiveness. Electronic reconfigurability brings another advantage to patch arrays since parabolic reflectors require mechanical scanning systems to change their main beam directions. However, microstrip arrays exhibit relatively high losses due to their complex feeding network especially at high frequencies. Additionally, spurious radiation from the feeding network may disturb the antenna performance. Therefore, reflectarray antennas [2] have been proposed to overcome these drawbacks.

A reflectarray is composed of a flat reflector and a feed antenna for the illumination. Planar reflector elements are printed on a dielectric substrate with a proper spacing without any RF feeding lines. Each element is designed to produce appropriate reflection phase values in order to achieve a planar phase surface in front of the aperture. Phase angles of elements are adjusted considering path lengths from the feed to an antenna element. Reflection elements can be microstrip patches where phase is adjusted by the length of a short section of feed line, or the reflection phase angle is adjusted by the shape and size of the element.

Electronic reconfigurability of reflectarrays is attained either by inserting a controllable phase shifter to each of their patch elements, e.g., phase shifters based on PIN diodes [3], varactor diodes [4] and MEMS devices [5], [6], or by directly controlling the resonances of patches with embedded RF components, e.g., PIN diodes [7], varactor diodes [8] and MEMS devices [9]. Alternatively, tunable substrates such as liquid crystals are used in reflectarrays to provide electronic reconfigurability [10]–[13]. The resonance of a patch element can be controlled by tuning the substrate to adjust the reflection phase angle of the element. Thus, the direction of the main beam can be controlled. Additionally, over the past few years, ferroelectric thick-film ceramics as a different sort of tunable substrate technology have been introduced on the basis of unit cell investigations [14], [15]. A review of reconfigurable reflectarrays has been done in [16] to examine the achievements that have been made in recent years.

Microstrip reflectarrays unite the parabolic reflector configuration and microstrip patch array technology. Therefore, they can exhibit an antenna performance close to parabolic reflectors in terms of high gain, low losses and low sidelobe levels especially for very large apertures [2]. Moreover, they possess the aforementioned advantages of microstrip array technology. However, the feed antenna configuration may be counted as a disadvantage for some applications with respect to antenna profile, and a feed antenna placed in front of the reflector leads to an aperture blockage. The aperture blockage is mitigated with an offset feed configuration, but the reflectarray still can not be qualified as a low-profile antenna. In this case, folded reflectarray antennas can provide an appropriate solution [17], [18].

Manuscript received February 08, 2013; revised September 18, 2013; accepted October 24, 2013. Date of publication November 05, 2014; date of current version December 31, 2014. This work was supported by the DFG-Project "Rekonfigurierbare Millimeterwellen-Antennen mit steuerbaren hoch-anisotropen Fluessigkristallen" under the project numbers JA 921/15 and ME 1016/14.

S. Bildik, C. Fritzsch, and R. Jakoby are with the Institute for Microwave Engineering and Photonics, Technische Universitaet Darmstadt, 64283 Darmstadt, Germany (e-mail: bildik@mwt.tu-darmstadt.de).

S. Dieter is with Cassidian, 85521 Ottobrunn, Germany.

W. Menzel is with the Institute of Microwave Techniques, University of Ulm, 89081 Ulm, Germany.

Color versions of one or more of the figures in this paper are available online at http://ieeexplore.ieee.org.

Digital Object Identifier 10.1109/TAP.2014.2367491

Their double reflector configuration decreases the antenna profile, leading to a higher compactness. Furthermore, the feed is integrated into the backside reflector, and consequently aperture blockage is significantly reduced.

Beam steering with folded reflectarrays has been realized so far by tilting the lower reflector with a mechanical system [19], by switching between several feeds placed at a certain spacing [20] or by using both methods to obtain two-dimensional beam steering [21]. The folded reflectarray antenna presented in this paper exploits the liquid crystal technology for the first time as an alternative method to provide a beam steering capability. A liquid crystal mixture has been utilized as a tunable substrate in the upper reflector to achieve this feature.

The antenna has been designed on the basis of works given in [20], [22], and [23]. The first one presents a modified polarizing grid that allows an offset beam by performing an additional phase angle adjustment on the upper reflector. In the second one, liquid crystal based reflectarray antenna technology for W-band has been established and the beam steering capabilities of the antenna has been demonstrated. A bifocal antenna design for reconfigurable folded reflectarrays and a concept of liquid crystal based polarizing grid has been discussed in the last one. In this work, a reconfigurable polarizing grid as an upper reflector has been realized, which has been derived from [22] considering the concept discussed in [23]. In order to achieve a relevant reconfigurable antenna design, the bifocal antenna design given in [20] has been modified in a way that all rays intersect in the center of the lower array as discussed in [23]. Moreover, a further modification process has been carried out considering the one-dimensional phase adjustment capability of the reconfigurable polarizing grid. After the fabrication of the folded reflectarray components, the upper reflector has been characterized to obtain the relation between the reflection phase angle and the bias voltage. Finally, both reflectors have been assembled according to the folded reflectarray configuration, and the beam steering capability of the liquid crystal based folded reflectarray antenna has been demonstrated as a proof of concept. The potential to achieve two-dimensional beam steering with this antenna has been also discussed.

II. Fundamentals of Liquid Crystal Based Microstrip Reflectarray Elements

Liquid crystals have been quite successful in display and photonic applications, and therefore they are well-known as optical components of LCD screens. Besides the optical region, characterizations of liquid crystals show that they also can be successfully used as a functional material in the microwave spectrum, beginning from 10 GHz [24]–[26].

Liquid crystals consist of elongated rod-like molecules and exhibit different electrical characteristics depending on how an RF field is incident on the molecules owing to anisotropy [27]. The orientation of a liquid crystal bulk can be changed by external electric or magnetic fields or by surface anchoring [27]. Therefore, a desired effective permittivity can be obtained if it is possible to control the bulk orientation. Thus, liquid crystals can be used as tunable substrates. They possess mesophases between solid and liquid states, i.e., crystal solid, smectic, nematic and isotropic liquid. The liquid crystal mixture used in this work

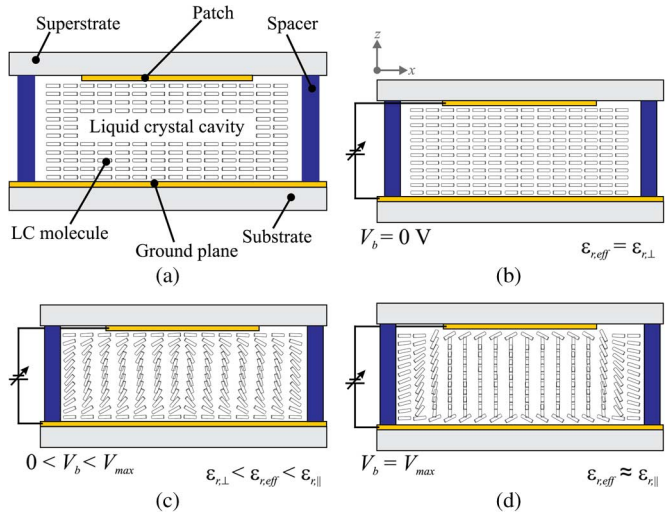

Fig. 1. Cross-section of the liquid crystal filled antenna element: (a) structure of the antenna element; (b) alignment of the liquid crystal bulk without a bias voltage; (c) with a bias voltage; and (d) with a saturation voltage .

is in the nematic phase, in which molecules have orientational order, but they do not have positional order yet.

The inverted microstrip line topology depicted in Fig. 1 can be used to build a tunable microstrip reflectarray element. The antenna element is composed of a substrate, a ground plane, a liquid crystal cavity, a microstrip patch and a superstrate [see Fig. 1(a)]. The upper part of the substrate is completely metalized to form the ground plane, and the patch is printed beneath the superstrate. The liquid crystal cavity is formed between the superstrate and the ground plane with the aid of spacers. It should be noted that the solid ground plane has been formed into a gridded structure in this work in order to adapt the liquid crystal based reflectarray element to the folded reflectarray concept.

The external electric field to control the bulk orientation can be maintained simply by applying a dc voltage between the patch and the ground plane. In the absence of a bias voltage or for the prealignment of the molecules, surface anchoring plays a part. In order to provide the anchoring effect, the ground plane and that side of the superstrate, where the patches are printed, are coated with a thin polyimide film. The polyimide layer is mechanically rubbed with a cloth so that tiny grooves are formed along the rubbing direction. Thus, the molecules are aligned along the grooves and become oriented parallel to the superstrate and the ground plane layers. In other words, without any bias voltage, molecules are perpendicular to the RF field between the patch and the ground plane. In this case, the effective relative permittivity of the liquid crystal bulk $(\varepsilon_{r,\text{eff}})$ is equal to $\varepsilon_{r,\perp}$ [see Fig. 1(b)]. As illustrated in Fig. 1(c), when a bias voltage (V_b) is applied, molecules begin to turn leading to a variation in the effective permittivity of the liquid crystal bulk. If the voltage is increased further, molecules orient along the bias field lines and parallel to the RF field and hence $\varepsilon_{r,\text{eff}}$ is almost equal to $\varepsilon_{r,||}$ [see Fig. 1(d)]. Relative permittivity and loss tangent values of the liquid crystal mixture (GT3-23001) used in this prototype antenna are presented in Table I according to the cases where molecules are perpendicular and parallel to

TABLE I
SPECIFICATIONS OF THE LIQUID CRYSTAL MIXTURE AT 30 GHz (23° C)

Mixture	$\varepsilon_{r,\perp}$	$\varepsilon_{r,\parallel}$	$\tan\delta_\perp$	$\tan\delta_\parallel$
GT3-23001	2.47	3.16	0.0151	0.0033

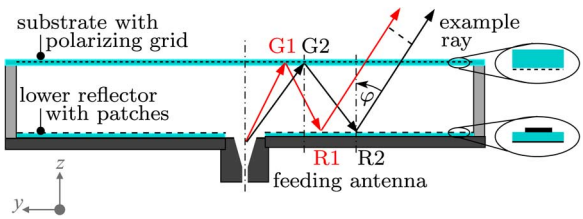

Fig. 2. Ray tracing principle of a folded reflectarray antenna for main beam direction φ and unit cell with polarizations.

the RF field. The electronically-controllable continuous permittivity variation as described above is used to obtain different reflection phase angle values in reconfigurable reflectarrays. Bias voltages are applied via thin bias lines that are connected to the reflecting elements. This biasing simplicity comes up as an advantage for the liquid crystal technology. In addition to that, the biasing of the liquid crystal based antenna element can be classified as low-power, since there is no need for any current flow through the element during the biasing.

III. Principle of a Folded Reflectarray Antenna

A folded reflectarray antenna as sketched in Fig. 2 consists of a lower planar reflector and an incorporated feed at the center. On top, there is an upper reflector, in the simple case a substrate with a printed metalized polarizing grid. The rays leave the central feed, are reflected at the polarizing grid of the upper reflector and passed back to the lower reflector. There, a phase angle correction takes place at the reflector elements in order to compensate for path length differences between the single rays. If the angle between the polarization of the incoming wave and the axes of the reflector element (square, dipole or rectangular patches) is set to 45°, the electric field vector can be decomposed into two components, and reflection properties of these components can be adjusted separately by changing the width and the length of the element [18]. The dimensions of elements are selected in a way that a phase angle difference of 180° is provided between the electric field components to twist the polarization of the incoming wave by 90°. Thus, a geometrical variation in two dimensions of the single reflector elements is used to both change the reflection phase angle of the incoming rays and to switch the polarization. Consequently, the rays can pass the polarizing grid of the upper reflector and leave the antenna in the desired direction.

This antenna type can be utilized for applications such as automotive radar [19], [28], object debris detection [29], or LMDS base stations [30]. It has been further developed, for instance, as a "multiple-beam" antenna for beam-steering in discrete steps [18], or as a folded antenna with an additional degree of freedom in the design by adding additional reflection elements to the upper reflector substrate [20]. The second method is modified in this publication for the ray tracing process described in Section IV-A.

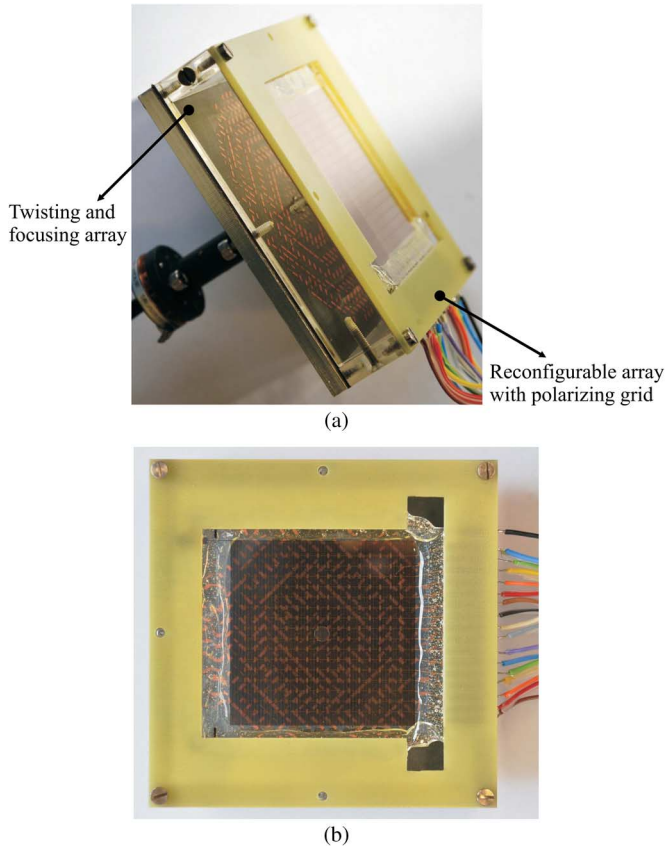

Fig. 3. Photograph of the realized reconfigurable folded reflectarray: (a) perspective and (b) top views.

IV. Antenna Design and Realization

The antenna presented in this paper is composed of an upper reflector based on liquid crystal technology, a static lower reflector fabricated with a conventional substrate and a circular waveguide feed horn placed at the center of the lower reflector. The upper reflector is a reconfigurable reflectarray with narrow reflector elements whose ground plane is replaced by a polarizing grid parallel to the reflector elements. The expected outcome of the prototype antenna is to maintain beam steering by using the continuous tunability of the liquid crystal based polarizing grid (upper reflector). Dimensions of the realized prototype antenna shown in Fig. 3 are $75\ \text{mm} \times 75\ \text{mm} \times 12\ \text{mm}$ representing length, width, and height, respectively. The height includes both the distance between reflectors and substrate thicknesses.

A. Ray Tracing Principle

The polarizing grid of the folded reflectarray antenna is combined in this work with a liquid crystal based reflector. In this way, in addition to a fixed phase angle adjustment and polarization twisting by the lower reflector, another degree of freedom is gained and used for beam steering. The basic underlying idea now is to redirect "rays" from an incident off-broadside direction back to the feed horn. As can be seen from Fig. 4, however, a direct implementation into a standard folded reflectarray leads to severe problems. Besides problems in the center area of the upper reflector, even for relatively small beam offset, only some

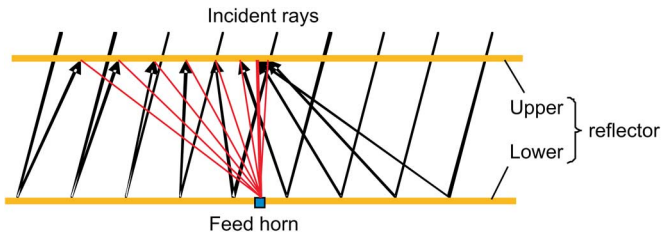

Fig. 4. Starting idea of beam steering with a "standard" folded reflectarray. An off-broadside receiving case is depicted. The red lines indicate the desired rays redirected by the upper reflector into the feed horn with the classical ray tracing method.

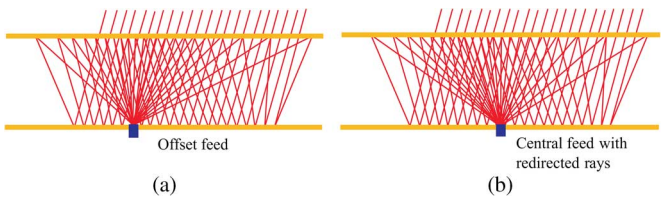

Fig. 5. (a) Ray tracing according to a bifocal antenna described in [20] and (b) modified redirection of rays to the centrally located feed.

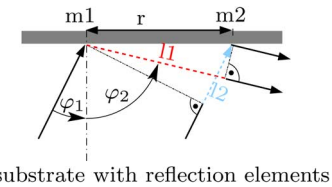

Fig. 6. Relation between incoming and reflected rays on a planar reflector.

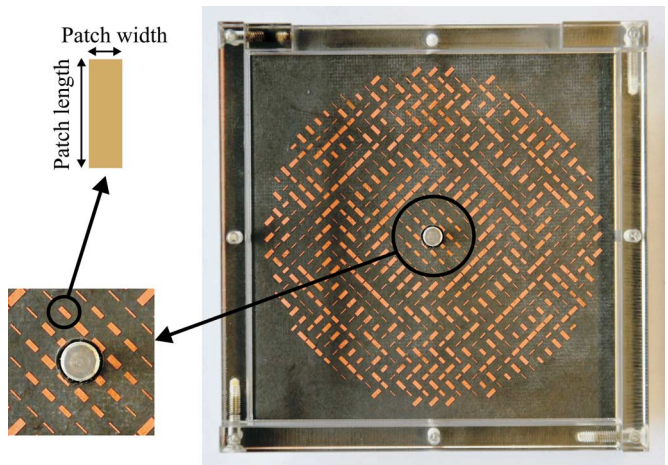

Fig. 7. Photograph of the realized twisting and focusing array.

parts of the upper reflector are involved resulting in considerable aperture efficiency reduction. This issue worsens especially for the transmit case in which the feed horn illuminates the complete upper reflector. The illumination of the areas without phase angle adjustment can spoil the radiation pattern especially by yielding higher sidelobes.

On the other hand, beam steering with multiple feeds has been demonstrated successfully in [20]. In this case, together with additional phase shifting properties of the upper reflector, also the lower reflector is modified based on the principle of bifocal antennas. In such antennas, the single focal point is replaced by a focal ring. Incident "rays" are distributed over a large part of the upper reflector, even for off-broadside incidence (see Fig. 5). Thus, all elements of the upper reflector can be used, in contrast to the situation depicted in Fig. 4. Now it is straightforward to redirect the rays to a feed and only the respective reflection condition has to be modified. However, the ray tracing process described in [20] is for an offset feed configuration [a lateral feed offset of 4 mm, see Fig. 5(a)]. Therefore, it has been modified for a central feed configuration by directing rays to the center of the lower reflector [see Fig. 5(b)]. This modification is related to the phase angle adjustment maintained by the upper reflector. Now the incident rays are reflected from the lower reflector in the same manner as in Fig. 5(a) but the upper reflector focuses all rays on the center of the lower reflector. This focusing action is electronically performed by tuning the liquid crystal substrate of the upper reflector according to main beam directions. Furthermore, the one-dimensional phase angle adjustment capability of the upper reflector has been considered and included in the ray tracing process. Thus, in order to collimate the beam, the lower reflector has a bifocal phase angle distribution in the plane shown in Fig. 5(b), and a parabolic phase angle distribution in the orthogonal plane.

The relation between incoming and outgoing rays as a function of incident and reflection angles is required for the ray tracing process. This relation is illustrated in Fig. 6. Two parallel incoming rays, which are separated by a small distance r, have an incident angle of φ_1 and a reflection angle of φ_2. m_1 and m_2 represent the electrical lengths added by antenna elements while $l_1 - l_2$ denote the path length difference. The relation is described by the formula

$$\frac{\partial m}{\partial r} = \sin(\varphi_2) - \sin(\varphi_1) \tag{1}$$

given in [20] and the reflection phase angle value α_i is connected with the electrical length m by

$$m_i = \frac{\alpha_i}{k_0}. \tag{2}$$

Considering the main beam direction, the feed position and the ray tracing shown in Fig. 5(b), which provides incident and reflection angles, required phase angle values of antenna elements are calculated by using (1) and (2). Substituting (2), incident and reflection angles (φ_1 and φ_2) in (1), and integrating it according to positions of the reflection elements, the required reflection phase angles α_i are obtained. These phase angle values are acquired by adjusting dimensions of the patches on the lower reflector, and by applying a bias voltage on the upper reflector.

B. Lower Reflector

In the approach used here, the substrate of the lower reflector (see Fig. 7) is Rogers 5880 with a thickness of 0.508 mm. The patch orientation on the reflector is rotated by 45° with respect to the grid orientation to achieve the polarization twisting [18]. Dimensions of the patches have been adjusted by changing both width and length to generate appropriate phase shifts and to switch the polarization. This has been performed by choosing

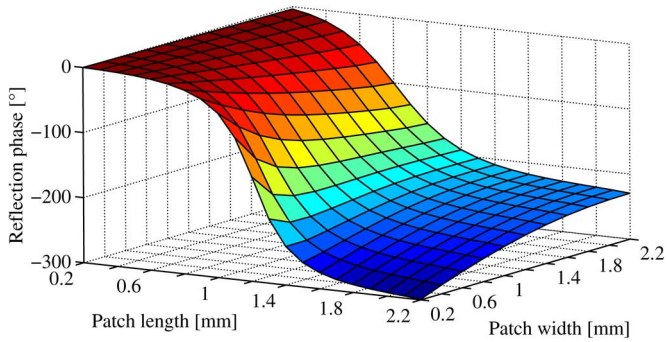

Fig. 8. Simulated reflection phase angle of lower reflector's unit cell as a function of length and width at 77 GHz (Cell size $= 2.25$ mm $\times$ 2.25 mm and $\varepsilon_r = 2.2$).

relevant dimensions from the simulation results presented in Fig. 8. Maximum reflection loss of 0.14 dB has been determined from the simulations.

The distance between both reflectors is 9 mm. To keep the feed horn diameter small (2.67 mm) and to adjust an optimal illumination of the upper reflector, a dielectric rod has been taken from the antenna described in [31]. Using this dielectric rod, its phase center is situated 2 mm above the reflector. Therefore, the effective feed horn distance is reduced by 2–16 mm, which was included in the ray tracing process. The amplitude taper at the edge of the lower reflector with a diameter of 36 mm is about 11 dB, which reduces losses due to spillover effects at the reflector edges.

C. Reconfigurable Array With Polarizing Grid

Similar to described in [20] or [23], the reconfigurable array (upper reflector) has to be transparent for one polarization and should reflect and adjust the respective phase angles for the other polarization. Therefore, the ground plane is realized as a grid. The reflector elements as narrow patches are parallel to the grid lines, while the bias lines are vertical [see Fig. 9(a)]. A required phase shift is generated by applying a bias voltage between a dipole and the gridded ground plane via bias lines, which are in contact with the dipoles. Furthermore, the reconfigurable array functions also as a radome for the folded reflectarray antenna.

Fused silica plates have been used as a superstrate and as a substrate with thicknesses of 300 and 600 μm, respectively. Using fused silica glasses is advantageous for the liquid crystal technology since they are mechanically and thermally stable, they exhibit very good chemical inertness, they have good optical and ultraviolet transparency, and they exhibit low RF losses. Mechanical stability plays an essential role to form a liquid crystal cavity with a uniform thickness. Exhibiting very low thermal expansion is significant for the reliability of the cavity sealing. Chemical inertness (except to hydrofluoric acid) establishes them as a proper material for chemical processes during the fabrication. Transparency is an advantage that maintains an efficient alignment for stacked layers, and it allows the inspection of the liquid crystal filling process. The loss tangent of the fused silica is below 0.0015 up to 90 GHz while the relative permittivity is 3.8 [32].

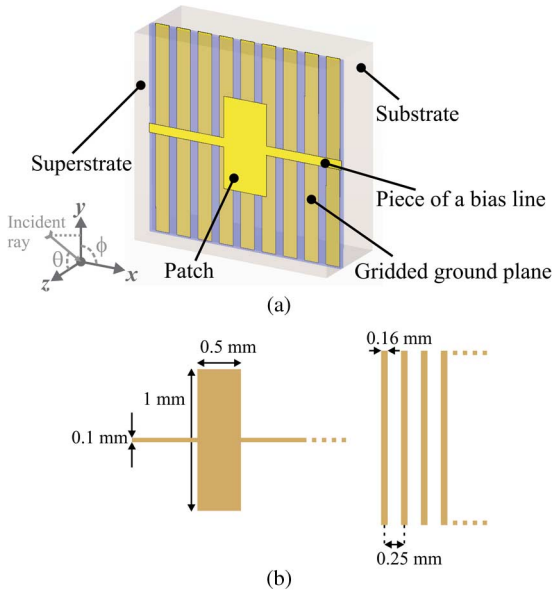

Fig. 9. (a) Designed unit cell of the reconfigurable array and (b) dimensions of the patch and the grid. (Cell size $= 2.25$ mm $\times$ 2.25 mm).

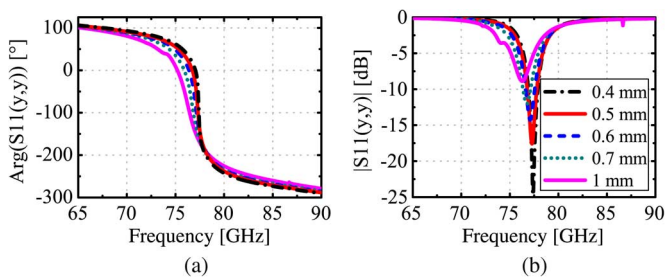

Fig. 10. Simulation results of the unit cell with different patch widths, where ε_r is 2.82: (a) reflection phase angle and (b) reflection amplitude.

The liquid crystal mixture used in this antenna has been characterized as described in [33]. Although the characterization was at 30 GHz, dielectric parameters presented in Table I have been used for the design of the reconfigurable array at W-band because the mixture's permittivity over frequency changes hardly beyond 10 GHz [24]–[26]. Therefore, the reconfigurable reflectarray presented in [22] has been successfully designed in a similar way.

Dimensions of the dipoles, the bias lines and the grid are illustrated in Fig. 9(b). The spacing between metallic lines of the grid has been chosen to be much smaller than the wavelength ($\sim \lambda_0/15$) in order to obtain a functional polarizing grid as well as an effective ground plane for the orthogonal polarization. The width of a grid line has been fine-tuned with a commercially available full-wave simulation software considering the reflection and the transmission in two orthogonal polarizations. The length of the dipole (in y-direction) has been set according to the operating frequency. The width has been optimized considering the reflection losses, the phase angle response and the required phase shift range, which is necessary for the beam steering action. Phase shift range of a unit cell can be extended if the width of the patch element is decreased. Thus, gaps in the phase angle adjustment can be reduced. As shown in Fig. 10(a), the phase

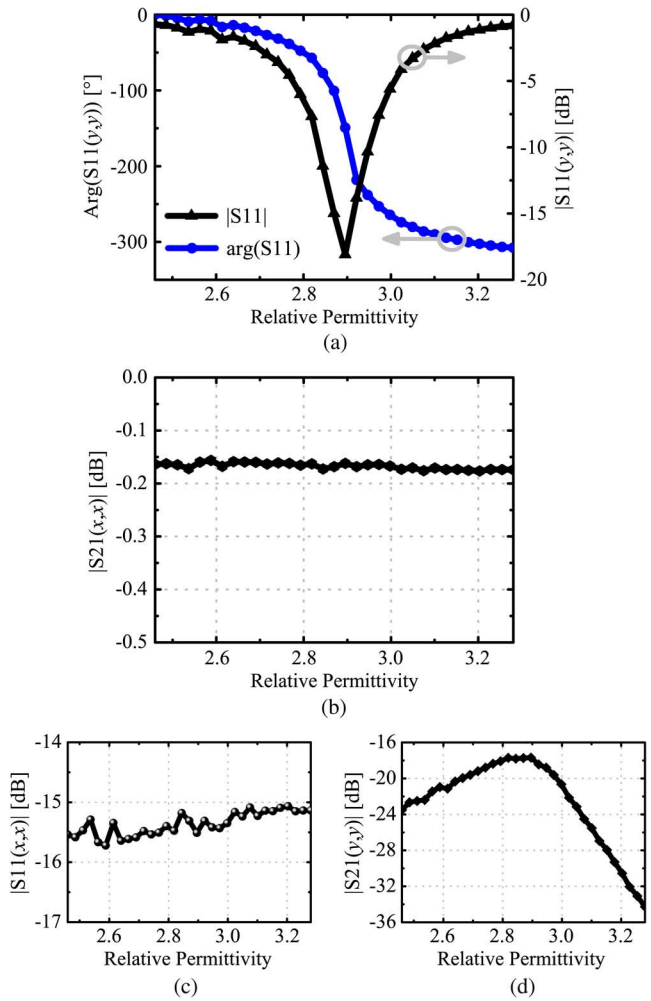

Fig. 11. Simulation results of the designed unit cell at 77 GHz: (a) desired reflection; (b) desired transmission; (c) unwanted reflection; and (d) unwanted transmission.

angle curve becomes longer and steeper when the width is reduced, which results in a greater differential phase shift. However, when the width is reduced more, e.g., to 0.4 mm, the phase angle curve becomes extremely steep at around 77 GHz. This case increases phase errors due to the fabrication tolerances and should be avoided. Additionally, as a trade-off, reflection losses increase while the width is narrowed to extend the phase angle range [see Fig. 10(b)]. These losses comprise dielectric loss, metal loss and surface wave loss. However, dielectric and metal losses are more significant than surface wave loss for a microstrip patch element with a low dielectric constant substrate [34]. It should be noted that dielectric and metal losses increase dramatically around the resonance frequency of the element because the electric field below the patch becomes stronger and the surface current on the patch rises. These two factors become much more significant when the width of the patch element is reduced [see Fig. 10(b)]. Moreover, since the used liquid crystal mixture has a greater loss tangent value compared to conventional RF substrates, the designed microstrip element exhibits relatively high losses.

S-parameter simulation results of a single antenna element can be seen in Fig. 11 versus relative permittivity. The reflection parameter of the waves polarized in y direction [see Fig. 9(a)] is denoted as $\mathrm{S11}(y,y)$, where the antenna element is illuminated in y-directed polarization. This is the required polarization to enable the reconfigurable array. By contrast, $\mathrm{S21}(y,y)$ represents the unwanted transmission of the waves that travel through the reconfigurable array in y-directed polarization. $\mathrm{S11}(x,x)$ represents the unwanted reflection in x-directed polarization when the antenna element is illuminated in the same polarization. The desired transmission is denoted as $\mathrm{S21}(x,x)$, where the illumination and the transmission are in x-directed polarization. According to the simulations, a single antenna element can generate a relative phase shift of about 305° within the given permittivity range while the maximum reflection loss is 18 dB [see Fig. 11(a)]. The simulated transmission loss for electric fields normal to the grid is less than 0.17 dB as can be seen in Fig. 11(b). Furthermore, the magnitude of the unwanted reflection is below -15 dB, and the unwanted transmission for fields parallel to the grid is below -17 dB. It should be noted that the loss tangent of the liquid crystal mixture has been fixed to 0.0151 $(\tan\delta_{\perp})$ to simplify the simulations. However, in reality, the loss tangent decreases from the perpendicular case to the parallel case (see Table I), which reduces the reflection loss of the antenna element. Additionally, owing to the resonant characteristics of microstrip dipole elements, reflection losses of each antenna element within the reconfigurable array will be different when they are biased with different voltages to obtain the required phase shifts.

In order to explicitly investigate the effect of the antenna elements with different amplitudes, radiation patterns of a 16×16 standard reflectarray have been calculated. The upper reflector of this work has been used as a single reflector for these calculations with an equal feed illumination. First of all, respective phase angle values of each reflectarray element have been calculated with a classical ray tracing process for the required main beam direction. The phase angle calculations have been performed for a center-fed configuration with an f/D ratio of 1 and an element spacing of $0.58\lambda_0$. The operating frequency has been set to 77 GHz. Amplitudes of each antenna element have been interpolated afterwards from the unit cell simulations shown in Fig. 11(a) by including the calculated phase angle values. Finally, radiation patterns have been calculated by using the obtained reflection amplitudes of the antenna elements. Amplitudes of the elements and radiation patterns of the reflectarray can be seen in Fig. 12 for a main beam direction of $-10°$. In these calculations not only the amplitude variations but also the phase angle gap due to the limited differential phase shift has been included. The 8th and the 9th array elements represent the central elements, and the 1st and the 16th elements represent the ones at the edges. A significant amplitude change from one element to another leads to distortion on the amplitude distribution over the array and consequently affects the array factor. Gain loss, main beam broadening and some pattern deformations can be seen in Fig. 12(b) as results of amplitude variation and losses. Especially first nulls almost disappear, and hence first sidelobes tend to merge with the main lobe. The asymmetry on the pattern results from the phase error, which is due to the limited differential phase shift.

The fabricated upper reflector, which is illustrated in Fig. 13, consists of 16×16 patch elements with an element spacing of

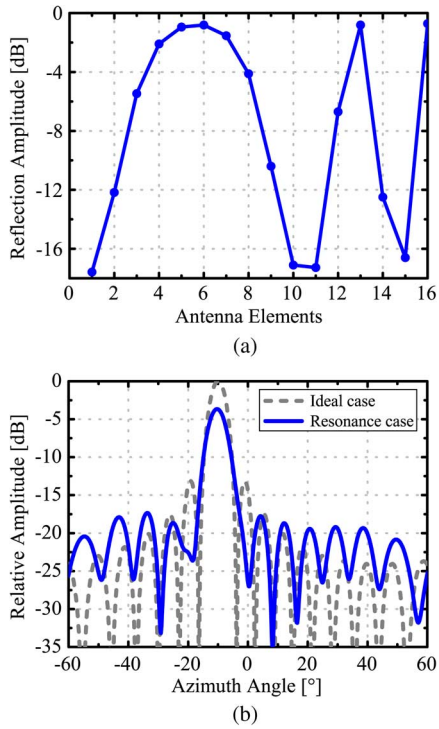

Fig. 12. (a) Simulated reflection amplitudes of the array elements in one column at 77 GHz when the main beam direction is $-10°$ and (b) calculated radiation patterns of a reflectarray with isotropic elements and equal feed illumination.

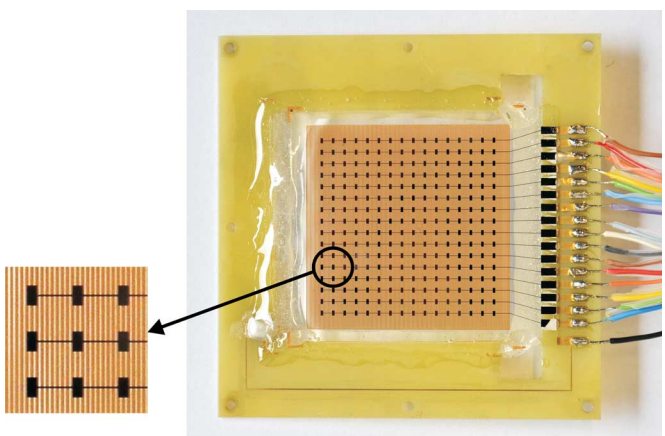

Fig. 13. Photograph of the realized liquid crystal based array with polarizing grid.

2.25 mm $(0.58\lambda_0)$. For the sake of simplicity, all 16 patches in the same row have been connected by the same bias line, thus providing the same phase shift and hence performing a one-dimensional beam scanning. The metallic structures on the superstrate and the substrate have been realized with Cr/Au deposition, photolithography, Au plating and Au/Cr etching processes, respectively. A thin polyimide film has been deposited onto the ground plane and the superstrate, and these layers have been rubbed for the prealignment of the liquid crystal bulk. In order to form the liquid crystal cavity, commercially available micro pearls with a diameter of 50 μm have been utilized as cavity spacers. These micro pearls have been mixed with glue and inserted between the two fused

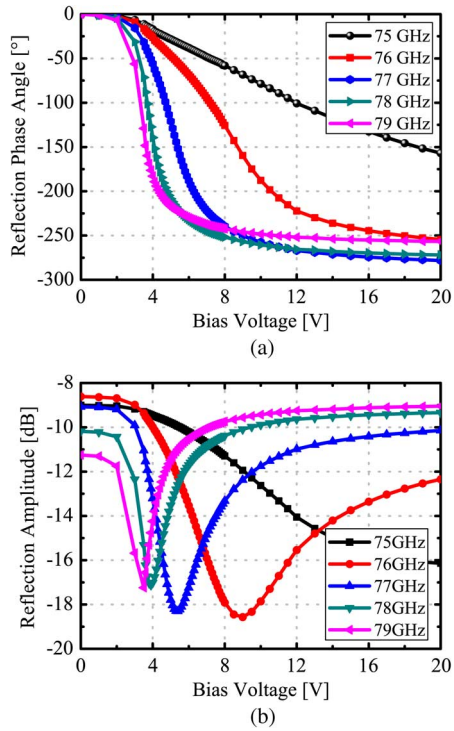

Fig. 14. (a) Measured relative phase shift and (b) reflection amplitude of the realized liquid crystal based array.

silica plates at locations outside the active region of the array to form a 50 μm-thick cavity. Wire bonding for the biasing circuitry connections, liquid crystal filling and hermetic sealing processes have been performed afterwards.

V. Measurements and Discussions

The antenna shown in Fig. 13 (upper reflector) has been characterized with a quasi-optical lens setup [35]. Measurements have been carried out by applying the same bias voltages (0–20 V) to each antenna element row. These measurement results have been normalized with measured results of a metallic plate, which has been placed at the same position of the antenna. Fig. 14(a) depicts the tuning capability of the realized upper reflector in terms of differential phase shift from 75 to 79 GHz. According to that measurement results, the antenna can generate more than 270° relative phase shift at 77 and 78 GHz. Minimum reflection amplitudes are -18.3 and -17.1 dB at 77 and 78 GHz, respectively [see Fig. 14(b)].

Fig. 15(a) presents the measured far-field patterns of the realized reconfigurable folded reflectarray (see Fig. 3) at 78 GHz for three different main beam directions. Sidelobe levels of -16.1, -8.9, and -6 dB are obtained for the beam directions of 0°, $-6°$, and 6°, respectively. The main beam for the broadside case has a hump-like shape at around $-6°$ and 6°, and the offset beam for $-6°$ has similar shape at around $-12°$. It seems that first sidelobes merged with the main beam in a way that this deformation is formed. As discussed in Section IV-C, this may occur due to amplitude changes from one element to another. However, since applied bias voltages for the broadside beam are all 0 V (see Table II), amplitudes of all elements are almost the same. They can differ only within fabrication tolerances, which

TABLE II
APPLIED BIAS VOLTAGE CONFIGURATIONS

Beam direction	**Bias voltage [V]**															
0°	0	0	0	0	0	0	0	0	0	0	0	0	0	0	0	0
−6°	4.46	2.91	0	15	0	3.17	4.12	5.05	6.12	11.80	0	4.04	5.22	7.09	15	4.10
6°	4.10	15	7.09	5.22	4.04	0	11.80	6.12	5.05	4.12	3.17	0	15	0	2.91	4.46
−17°	9	6.56	0	15	3.98	5.21	0	4.08	10.54	13	0	0	2.66	0	13	4.38
Row numbers:	1	2	3	4	5	6	7	8	9	10	11	12	13	14	15	16

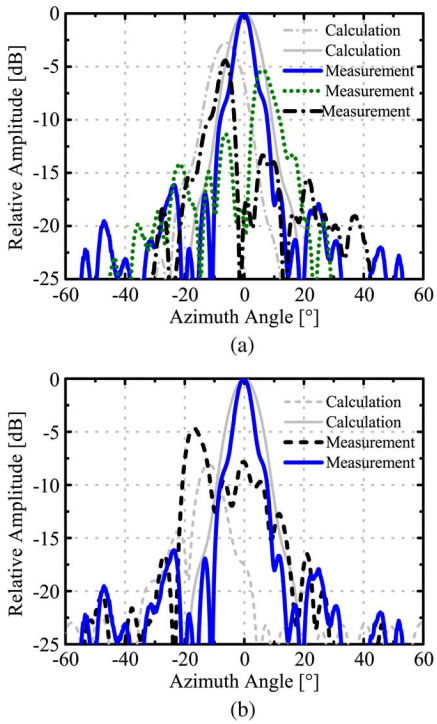

Fig. 15. Measured radiation patterns of the reconfigurable folded reflectarray antenna at 78 GHz together with the respective calculated patterns: (a) main beam at −6°, 0°, and 6°, and (b) main beam at −17° and 0°. Calculated radiation patterns have been obtained considering the feed illumination, applied bias voltages, and thereby measured reflection amplitudes and phase angle gaps of the upper reflector.

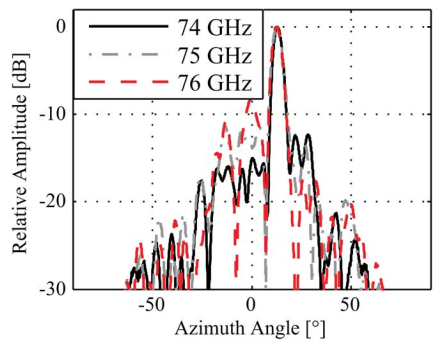

Fig. 16. Measured radiation patterns of the folded antenna with a modified grid for an offset beam design ($\varphi = 15°$), based on a common RF substrate.

can not be that much severe. Therefore, feed illumination and edge effects (due to illumination of the upper reflector's edges) should be also taken into account as another factor that leads to the aforementioned pattern deformation.

Power differences between the electronically scanned patterns result from the resonant characteristics of upper reflector's elements (see Fig. 11(a) and Fig. 12). Depending on the bias voltage configuration, the fewer number of elements with higher losses the antenna has, the less power drop it exhibits. As mentioned before, applied bias voltages for the broadside case are all 0 V. Therefore, the elements are out of resonance that leads to lower losses. However, for the offset beams, many elements are at resonance resulting in higher losses and consequently gain loss. This can be seen in Fig. 12(b) with the comparison of patterns for ideal case and for elements with resonance.

The voltage configurations have been derived from the ray tracing procedure mentioned in Section IV-A, including the antenna characteristics from the quasi-optical measurement results. They are presented in Table II. The configuration of the offset beam for 6° has been obtained by flipping the voltage order for the −6° offset beam.

When the main beam is steered to −17°, a sidelobe at 0° arises that leads to a deterioration in the radiation pattern of the antenna [see Fig. 15(b)]. The same phenomenon occurs when the reconfigurable upper reflector is replaced with an untunable one. This untunable grid is composed of a conventional RF substrate with a metallic grid and patches, which are printed on the opposite surfaces of the substrate. The offset beam is obtained by performing an additional phase angle adjustment with the patches on the upper reflector. As shown in Fig. 16, the sidelobe at 0° becomes smaller at 74 GHz resulting in a better radiation pattern on the one hand, although the main reflector is designed at a central operating frequency of 77 GHz. Besides the fabrication tolerances, this may result from also standing waves between the two reflectors, which are affected by frequency changes. The standing waves can be generated by spurious reflections from the ground planes of reflectors and by reflections due to transmission mismatches. On the other hand, the best radiation patterns of the reconfigurable folded reflectarray are obtained at 78 GHz, instead of 74 GHz, because the tuning capability of the upper reflector is better in the range of 77–78 GHz, which can be seen from the differential phase shift in Fig. 14.

In order to mitigate the effects of this phenomenon, an antenna element with a broader bandwidth may be used. For instance, coupled microstrip dipole configurations given in [13], [22] exhibit broader bandwidth and larger differential phase shift. The second work has shown that a relative phase shift of 300° (at least) can be yielded at 6 GHz frequency interval while the bias voltage is changed from 0 to 15 V [36]. Thus, gaps in the phase angle adjustment during the shift of the operating

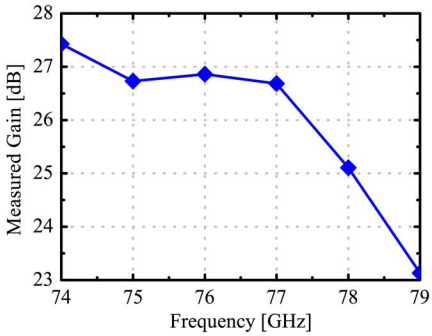

Fig. 17. Measured antenna gain from 74 to 79 GHz.

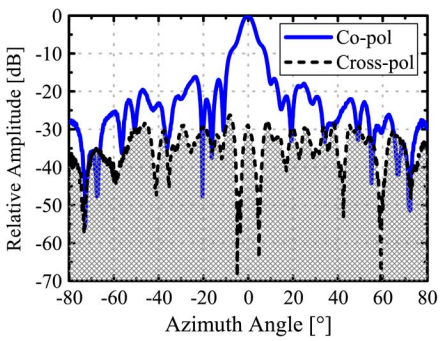

Fig. 18. Measured far-field radiation patterns in co- and cross-polarization at 78 GHz.

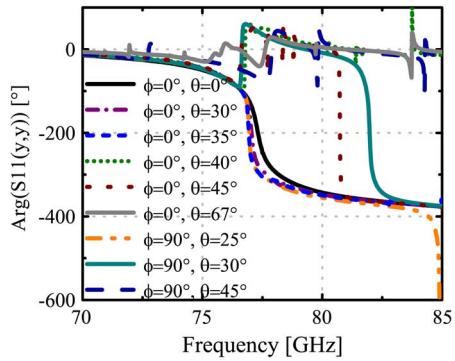

Fig. 19. Simulation results of the liquid crystal based unit cell with different angle of incidences (from normal incidence to the maximum incidence angle 67°).

frequency can be narrowed or completely avoided. Furthermore, using an antenna pattern synthesis method, e.g., based on particle swarm optimization [22], [37], which includes characterization measurements of the upper reflector and the feed, may improve the radiation patterns. This optimization method should be used with aforementioned broadband elements to be efficient and hence especially the power difference between the electronically scanned patterns can be reduced [36].

The measured gain of the realized antenna, where the main beam is at 0°, is 25.1 dB at 78 GHz as shown in Fig. 17. The antenna gain increases toward 74 GHz, which can be explained by the aforementioned issue.

Since the realized antenna comprises a polarizing grid and is a center-fed configuration, low cross-polarization levels are expected. The cross-polarization in Fig. 18 has been measured at all angular directions. It has a peak value of -26.2 dB and a mean value of -35.6 dB.

Another parameter that affects the antenna performance is the angle of incidence at antenna elements. The performance of the liquid crystal based antenna element is illustrated in Fig. 19 according to different incident angles. As can be seen in the figure, the phase angle curve of the element is distorted after $\phi = 0^\circ$ $\theta = 40^\circ$ and $\phi = 90^\circ$ $\theta = 30^\circ$. At 78 GHz, phase angle deviations compared to normal incidence are -22.2°, -29.6°, and -41.5° for the incident angles of $\phi = 0^\circ$ $\theta = 35^\circ$, 40°, and 67°, respectively. For $\phi = 90^\circ$ $\theta = 25^\circ$, 30°, and 45°, phase angle deviations are -29.6°, -46.7°, and -31.6°, respectively. The effect of oblique incidence can be mitigated by decreasing the element spacing and by enlarging the width of the dipoles. However, if the dipoles are widened, the differential phase shift of the antenna elements decreases. Therefore, a coupled dipole configuration can be a proper solution also for this issue owing to its larger differential phase shift capacity. Thus, this configuration can mitigate the effect, as well as exhibit the required larger differential phase shift [13]. Furthermore, a two-dimensional reconfigurable antenna design with a pattern optimization method can be another or supporting solution for this effect because in this way each antenna element can be optimized individually and hence phase errors can be reduced or completely corrected.

Two-dimensional beam steering can be achieved if antenna elements are biased individually. A liquid crystal based reflectarray prototype, which has been designed for this purpose, has been presented in [38]. Ground planes of each unit cell have been separated by etching a fine grid on the solid ground plane. Consequently, the ground planes are isolated with small gaps. Thus, each unit cell possesses its own ground to apply separate bias voltages. Each row of patches, which have been connected by respective bias lines as done in this work, have been interconnected to apply a bias voltage between patches and ground elements. The connection between the ground sections and the biasing circuitry has been maintained with metallic vias, which have been formed through the substrate. A modification is necessary to apply this concept to the antenna presented in this paper because the ground plane is already composed of a gridded structure (polarizing grid). After the isolation of ground sections with small gaps, the metallic structures of an individual gridded ground plane should be interconnected by a thin line to provide the same electrical potential (see Fig. 20). Bias lines, which are connected to the gridded ground structures with vias, can be printed on the other side of the substrate over the metallic lines of the grid. These bias lines should be placed properly to avoid a blockage over the polarizing grid. If they are printed as shown in Fig. 20, their effect on the antenna performance can be neglected according to simulation results. All bias lines, especially the ones at the active region of the antenna, can be realized by using high-resistivity materials, e.g., indium–tin–oxide (ITO), instead of Au to mitigate RF interference, as utilized in [39] to bias a liquid crystal based ring resonator. Alternatively, separate bias lines can be printed on the superstrate and directly connected to patches in order to bias antenna elements individually. Considering the presence of this bias lines at the active region of the antenna, a proper

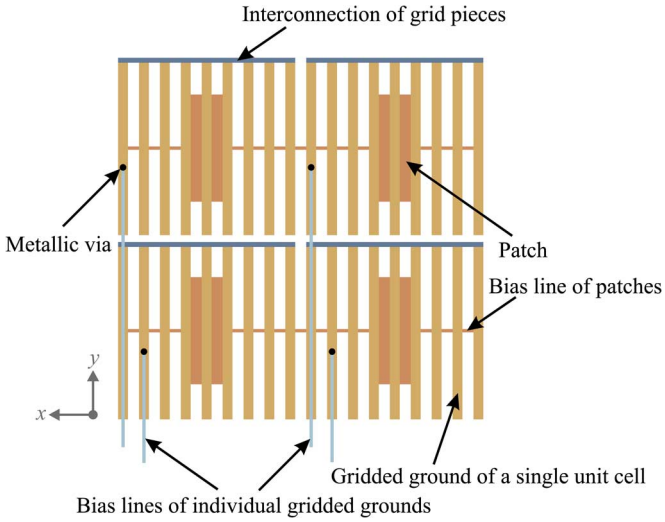

Fig. 20. Proposed biasing layout of separate grounds for two-dimensional beam steering. Four unit cells are depicted as an example. The layout can be extended according to the array configuration. The gridded grounds and their bias lines are printed on the opposite surfaces of the substrate. Their connections are maintained by metallic vias.

bias line layout is necessary and materials such as ITO should be used to avoid RF blockage.

VI. Conclusion

A liquid crystal based folded reflectarray antenna with the features of reconfigurability, high gain and low profile has been presented. The purpose to exploit the liquid crystal technology was to obtain electronic reconfigurability, continuous tunability and low-power biasing. The beam steering capability of the antenna has been demonstrated by steering the main beam to $-6°$, $0°$, and $6°$. The measured gain of the antenna is 25.1 dB at 78 GHz. The cross-polarization suppression measured at $0°$ angular direction is 29.7 dB.

Fabrication technology of the proposed antenna combines liquid crystal display and printed circuit board technologies. Therefore, arrays with many elements can be fabricated with a simple and low-cost automated manufacturing technique. Such an antenna can be utilized for applications such as automotive radar, 60 GHz wireless local area communication, or LMDS services.

Two-dimensional beam steering can be obtained if a proper bias line layout is designed. An antenna pattern synthesis method, e.g., based on particle swarm optimization, which includes characterization measurements of the upper reflector and the feed, may be used to improve the radiation patterns.

Acknowledgment

The authors would like to thank Merck KGaA for providing the employed liquid crystals, and CST GmbH for providing CST Microwave Studio.

References

[1] D. M. Pozar and D. Schaubert, "Microstrip Antenna Array Design," in *Microstrip Antennas: The Analysis and Design of Microstrip Antennas and Arrays*. New York, NY, USA: Wiley–IEEE Press, 1995, pp. 267–308.

[2] J. Huang and J. A. Encinar, "Introduction to reflectarray antenna," in *Reflectarray Antennas*. Hoboken, NJ, USA: Wiley, 2007, pp. 1–7.

[3] E. Carrasco, M. Barba, and J. Encinar, "X-band reflectarray antenna with switching-beam using PIN diodes and gathered elements," *IEEE Trans. Antennas Propag.*, vol. 60, no. 12, pp. 5700–5708, Dec. 2012.

[4] M. Riel and J.-J. Laurin, "Design of an electronically beam scanning reflectarray using aperture-coupled elements," *IEEE Trans. Antennas Propag.*, vol. 55, no. 5, pp. 1260–1266, May 2007.

[5] B. Mencagli, R. Gatti, L. Marcaccioli, and R. Sorrentino, "Design of large mm-wave beam-scanning reflectarrays," in *Proc. Eur. Microw. Conf.*, 2005, pp. 475–478.

[6] O. Bayraktar, O. Civi, and T. Akin, "Beam switching reflectarray monolithically integrated with RF MEMS switches," *IEEE Trans. Antennas Propag.*, vol. 60, no. 2, pp. 854–862, Feb. 2012.

[7] H. Kamoda, T. Iwasaki, J. Tsumochi, and T. Kuki, "60-GHz electrically reconfigurable reflectarray using p-i-n diode," in *IEEE MTT-S Int. Microw. Symp. Dig.*, 2009, pp. 1177–1180.

[8] S. Hum, M. Okoniewski, and R. Davies, "Realizing an electronically tunable reflectarray using varactor diode-tuned elements," *IEEE Microw. Wireless Compon. Lett.*, vol. 15, no. 6, pp. 422–424, 2005.

[9] C. Guclu, J. Perruisseau-Carrier, and O. Civi, "Proof of concept of a dual-band circularly-polarized RF MEMS beam-switching reflectarray," *IEEE Trans. Antennas Propag.*, vol. 60, no. 11, pp. 5451–5455, Nov. 2012.

[10] R. Marin, A. Mossinger, J. Freese, A. Manabe, and R. Jakoby, "Realization of 35 GHz steerable reflectarray using highly anisotropic liquid crystal," in *Proc. IEEE Antennas Propag. Soc. Int. Symp.*, 2006, pp. 4307–4310.

[11] A. Moessinger, R. Marin, S. Mueller, J. Freese, and R. Jakoby, "Electronically reconfigurable reflectarrays with nematic liquid crystals," *Electron. Lett.*, vol. 42, no. 16, pp. 899–900, Aug. 2006.

[12] W. Hu, M. Ismail, R. Cahill, J. Encinar, V. Fusco, H. Gamble, D. Linton, R. Dickie, N. Grant, and S. Rea, "Liquid-crystal-based reflectarray antenna with electronically switchable monopulse patterns," *Electron. Lett.*, vol. 43, no. 14, Jul. 5, 2007.

[13] G. Perez-Palomino, P. Baine, R. Dickie, M. Bain, J. Encinar, R. Cahill, M. Barba, and G. Toso, "Design and experimental validation of liquid crystal-based reconfigurable reflectarray elements with improved bandwidth in F-band," *IEEE Trans. Antennas Propag.*, vol. 61, no. 4, pp. 1704–1713, Apr. 2013.

[14] M. Sazegar, A. Giere, Y. Zheng, H. Maune, A. Moessinger, and R. Jakoby, "Reconfigurable unit cell for reflectarray antenna based on barium-strontium-titanate thick-film ceramic," in *Proc. Eur. Microw. Conf.*, 2009, pp. 598–601.

[15] Y. Shen, S. Ebadi, P. Wahid, and X. Gong, "Tunable reflectarray unit cell element using BST technology," in *Proc. IEEE Radio Wireless Symp. (RWS)*, 2012, pp. 43–46.

[16] S. Hum and J. Perruisseau-Carrier, "Reconfigurable reflectarrays and array lenses for dynamic antenna beam control: A review," *IEEE Trans. Antennas Propag.*, vol. 62, no. 1, pp. 183–198, Jan. 2014.

[17] D. Pilz and W. Menzel, "Folded reflectarray antenna," *Electron. Lett.*, vol. 34, no. 9, pp. 832–833, 1998.

[18] W. Menzel, D. Pilz, and M. Al-Tikriti, "Millimeter-wave folded reflector antennas with high gain, low loss, and low profile," *IEEE Antennas Propag. Mag.*, vol. 44, no. 3, pp. 24–29, Jun. 2002.

[19] W. Menzel, D. Pilz, and R. Leberer, "A 77-GHz FM/CW radar front-end with a low-profile low-loss printed antenna," *IEEE Trans. Microw. Theory Techn.*, vol. 47, no. 12, pp. 2237–2241, Dec. 1999.

[20] W. Menzel, M. Al-Tikriti, and R. Leberer, "A 76 GHz multiple-beam planar reflector antenna," in *Proc. 32nd Eur. Microw. Conf.*, 2002, pp. 1–4.

[21] W. Menzel and D. Kessler, "A folded reflectarray antenna for 2D scanning," in *Proc. German Microw. Conf.*, 2009, pp. 1–4.

[22] S. Bildik, S. Dieter, C. Fritzsch, M. Frei, C. Fischer, W. Menzel, and R. Jakoby, "Reconfigurable liquid crystal reflectarray with extended tunable phase range," in *Proc. 41st Eur. Microw. Conf. (EuMC)*, Oct. 2011, pp. 1292–1295.

[23] S. Dieter, P. Feil, and W. Menzel, "Folded reflectarray antenna using a modified polarization grid for beam-steering," in *Proc. 5th Eur. Conf. Antennas Propag.*, 2011, pp. 1400–1403.

[24] S. Mueller, A. Penirschke, C. Damm, P. Scheele, M. Wittek, C. Weil, and R. Jakoby, "Broad-band microwave characterization of liquid crystals using a temperature-controlled coaxial transmission line," *IEEE Trans. Microw. Theory Techn.*, vol. 53, no. 6, pp. 1937–1945, Jun. 2005.

[25] S. Bulja, D. Mirshekar-Syahkal, R. James, S. Day, and F. Fernadez, "Measurement of dielectric properties of nematic liquid crystals at millimeter wavelength," *IEEE Trans. Microw. Theory Techn.*, vol. 58, no. 12, pp. 3493–3501, Dec. 2010.
[26] S. Mueller, F. Goelden, P. Scheele, M. Wittek, C. Hock, and R. Jakoby, "Passive phase shifter for W-band applications using liquid crystals," in *Proc. 36th Eur. Microw. Conf.*, Sep. 10–15, 2006, pp. 306–309.
[27] D.-K. Yang and S.-T. Wu, "Liquid Crystal Physics," in *Fundamentals of Liquid Crystal Devices*. Hoboken, NJ, USA: Wiley, 2006, pp. 1–37.
[28] P. Feil, W. Mayer, and W. Menzel, "A 77 GHz eight-channel shaped beam planar reflector antenna," in *Proc. 3rd Eur. Conf. Antennas Propag.*, 2009, pp. 1320–1323.
[29] P. Feil, A. Zeitler, T. P. Nguyen, C. Pichot, C. Migliaccio, and W. Menzel, "Foreign object debris detection using a 78 GHz sensor with cosec antenna," in *Proc. Eur. Radar Conf.*, 2010, pp. 33–36.
[30] J. A. Zornoza, R. Leberer, J. A. Encinar, and W. Menzel, "Folded multilayer microstrip reflectarray with shaped pattern," *IEEE Trans. Antennas Propag.*, vol. 54, no. 2, pp. 510–518, Feb. 2006.
[31] T. P. Nguyen, C. Pichot, C. Migliaccio, and W. Menzel, "Study of folded reflector multibeam antenna with dielectric rods as primary source," *IEEE Antennas Wireless Propag. Lett.*, vol. 8, pp. 786–789, 2009.
[32] D. Liu, "Antenna Design for 60 GHz Packaging Applications," in *Advanced Millimeter-Wave Technologies: Antennas, Packaging and Circuits*. Hoboken, NJ, USA: Wiley, 2009, pp. 295–351.
[33] F. Goelden, A. Lapanik, A. Gaebler, S. Mueller, W. Haase, and R. Jakoby, "Systematic investigation of Nematic liquid crystal mixtures at 30 GHz," in *Proc. IEEE/LEOS Summer Topical Meet.*, 2007, pp. 202–203.
[34] D. M. Pozar, S. D. Targonski, and H. D. Syrigos, "Design of millimeter wave microstrip reflectarrays," *IEEE Trans. Antennas Propag.*, vol. 45, no. 2, pp. 287–296, Feb. 1997.
[35] A. Moessinger, S. Dieter, W. Menzel, S. Mueller, and R. Jakoby, "Realization and characterization of a 77 GHz reconfigurable liquid crystal reflectarray," in *Proc. 13th Int. Symp. Antenna Technol. Appl. Electromagn., Canadian Radio Sci. Meet.*, Feb. 15–18, 2009, pp. 1–4.
[36] S. Bildik, O. H. Karabey, S. Dieter, C. Fritzsch, A. Gaebler, R. Jakoby, and W. Menzel, "Recent advances on liquid crystal based reconfigurable antenna arrays," presented at the ESA Workshop on Large Deployable Antennas, Noordwijk, The Netherlands, Oct. 2012.
[37] S. Dieter, C. Fischer, and W. Menzel, "Design of a folded reflectarray antenna using particle swarm optimization," in *Proc. Eur. Microw. Conf.*, Sep. 28–30, 2010, pp. 731–734.
[38] A. Moessinger, S. Dieter, R. Jakoby, W. Menzel, and S. Mueller, "Reconfigurable LC-reflectarray setup and characterisation," in *Proc. 3rd Eur. Conf. Antennas Propag.*, 2009, pp. 2761–2765.
[39] A. Moessinger, C. Fritzsch, S. Bildik, and R. Jakoby, "Compact tunable Ka-band phase shifter based on liquid crystals," in *IEEE MTT-S Int. Microw. Symp. Dig.*, 2010, pp. 1020–1023.

Saygin Bildik (S'08–M'12) was born in Izmir, Turkey in 1983. He received the B.Sc. degree in electrical and electronics engineering from Ege University, Izmir, Turkey, in 2005, and the M.Sc. degree in electrical and electronics engineering from the Izmir Institute of Technology, Izmir, Turkey in 2008. He is currently working toward the Ph.D. degree in reconfigurable antennas at Technische Universitaet Darmstadt, Darmstadt, Germany.

He has been with Rohde & Schwarz, Munich, Germany, since 2014. His research interests are mainly in reconfigurable reflectarrays based on liquid crystals.

Mr. Bildik received the EuMC Young Engineer Prize from European Microwave Association within the conference European Microwave Week 2011.

Sabine Dieter (S'08–M'11) received the Dipl.-Ing. degree from the University of Ulm, Germany in 2007.

From 2007 to 2011, she was with the Institute of Microwave Techniques, University of Ulm, Ulm, Germany, as a Research Assistant, in the field of antenna design, optimization, and characterization. She has been with Cassidian, Ottobrunn, Germany, since 2012.

Carsten Fritzsch (S'08) received the diploma in electrical engineering from Technische Universität Darmstadt, Darmstadt, Germany, in 2008, and is currently working toward the Ph.D. degree at the Institute for Microwave Engineering and Photonics of the same university.

He is with Merck, Darmstadt, Germany, since 2014. His current research interests include reconfigurable antennas and components based on liquid crystals, and related fabrication and measurement technologies.

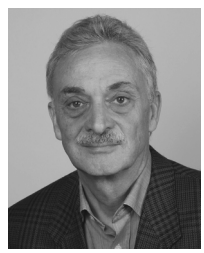

Wolfgang Menzel (M'89–SM'90–F'01) received the Dipl.-Ing. degree in electrical engineering from the Technical University of Aachen, Aachen, Germany, in 1974, and the Dr.-Ing. degree from the University of Duisburg, Duisburg, Germany, in 1977.

From 1979 to 1989, he was with the Millimeter-Wave Department, AEG, Ulm, Germany [now the European Aerospace, Defense, and Space Systems (EADS)], and was promoted to Head of the department. In 1989, he became a Full Professor with the Institute of Microwave Techniques, University of Ulm, Germany. His current areas of interest are multilayer planar circuits, waveguide filters and components, antennas, millimeter-wave and microwave interconnects and packaging, and millimeter-wave application and system aspects.

Rolf Jakoby (M'97) was born in Kinheim, Germany, in 1958. He received the Dipl.-Ing. and Dr.-Ing. degrees in electrical engineering from the University of Siegen, Siegen, Germany, in 1985 and 1990, respectively.

In January 1991, he joined the Research Center of Deutsche Telekom in Darmstadt, Germany. Since April 1997 he has a full professorship at TU Darmstadt, Germany. He is coinventor of nine patents and participates on eleven awards in the last six years. His interdisciplinary research is focused on RFID, micro- and millimeter wave detectors and sensors for various applications, and in particular on reconfigurable RF passive devices by using novel approaches with metamaterial structures, liquid crystal, and ferroelectric thick/thin film technologies.

Dr. Jakoby is a member of the Society for Information Technology (ITG) of the VDE and a member of the IEEE societies MTT and AP. He is organizer of various workshops, member of various TPCs, and has been Chairman of the European Microwave Conference 2007 and the German Microwave Conference 2011. He is Editor-in-Chief of "FREQUENZ." In 1992, he received an award from the CCI Siegen, and in 1997, the ITG-Prize for an excellent publication in the IEEE TRANSACTIONS ON ANTENNAS AND PROPAGATION.